

Theoretical Study of New Acceptor and Donor Molecules based on Polycyclic Aromatic Hydrocarbons

S. Shahab Naghavi, Thomas Gruhn, Vajiheh Alijani, Gerhard H. Fecher, Claudia Felser

*Institut für Anorganische Chemie und Analytische Chemie,
Johannes Gutenberg - Universität, 55099 Mainz, Germany**

Katerina Medjanik, Dmytro Kutnyakhov, Sergej A. Nepijko, Gerd Schönhense

Institut für Physik, Johannes Gutenberg - Universität, 55099 Mainz, Germany

Ralph Rieger, Martin Baumgarten, Klaus Müllen

*Max-Planck-Institut für Polymerforschung,
Ackermannweg 10, 55128 Mainz, Germany*

(Dated: May 22, 2018)

Abstract

Functionalized polycyclic aromatic hydrocarbons (PAHs) are an interesting class of molecules in which the electronic state of the graphene-like hydrocarbon part is tuned by the functional group. Searching for new types of donor and acceptor molecules, a set of new PAHs has recently been investigated experimentally using ultraviolet photoelectron spectroscopy (UPS). In this work, the electronic structure of the PAHs is studied numerically with the help of B3LYP hybrid density functionals. Using the Δ SCF method, electron binding energies have been determined which affirm, specify and complement the UPS data. Symmetry properties of molecular orbitals are analyzed for a categorization and an estimate of the related signal strength. While σ -like orbitals are difficult to detect in UPS spectra of condensed film, calculation provides a detailed insight into the hidden parts of the electronic structure of donor and acceptor molecules. In addition, a diffuse basis set (6-311++G**) was used to calculate electron affinity and LUMO eigenvalues. The calculated electron affinity (EA) provides a classification of the donor/acceptor properties of the studied molecules. Coronene-hexaone shows a high EA, comparable to TCNQ, which is a well-known classical acceptor. Calculated HOMO-LUMO gaps using the related eigenvalues have a good agreement with the experimental lowest excitation energies. TD-DFT also accurately predicts the measured optical gap.

Keywords: PAHs, charge transfer complex, electron binding energy, vertical ionization, Koopmans' theorem, UPS, electron affinity

* naghavi@uni-mainz.de

I. INTRODUCTION

Charge transfer salts have become of particular interest during the past two decades, in which both the interest in electronics on the molecular scale as well as the methods of chemical synthesis has strongly increased. Typically, charge transfer (CT) complexes, consisting of π -electron donors (D) and acceptors (A), show one or several properties like metallic conductivity, superconductivity, and magnetism that are relevant for nanoelectronic applications [1, 2]. Many of the organic conductors and superconductors are based on the bis(ethylenedithio)tetrathiafulvalene (BEDT-TTF) donor and various acceptors [2, 3]. Furthermore, poly cyano derivatives have mainly been used as acceptors like tetracyanoquinodimethane (TCNQ) [4]. Recently, a novel type of donor and acceptor molecules based on polycyclic aromatic hydrocarbons (PAHs) has been investigated [5]. In this article, a detailed numerical study of the electronic properties of new PAHs is presented, which allows to identify the experimental results and complements the picture of experimentally determined orbital states.

Flat aromatic molecules as polycyclic aromatic hydrocarbons (PAHs), have attracted attention because of their extended π -electron systems [6, 7]. Garito and Heeger concluded that the extension of the π system would lead to a lowering of intramolecular Coulomb repulsion in the anions of the acceptors, resulting in more stable radical anions and in highly conducting CT complexes [8]. Larger PAH molecules called nanographene have been synthesized in the bottom-up approach with desired size, structure, and symmetry [9]. The electronic structure of PAHs can be tuned via the type and number of substitutions in periphery. This way the functionalized PAHs may serve as a prototype for the creation of a new class of molecules with tailored chemical and electronic properties. However, although the electronic structure of different donor and acceptor molecules have been widely studied, little attention has been paid by theory and experiment to illustrate the electronic structure and the effect of functional groups on donors and acceptors based on PAHs.

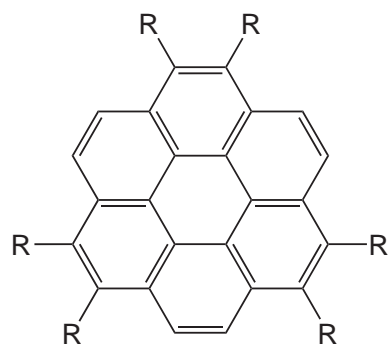
In this study we calculate the electronic structure of new acceptors and donors based on coronene and pyrene (see Fig. 1). A hybrid density functional (B3LYP) method is used to calculate the ionization potentials (IPs). The results are compared with ultraviolet photoelectron spectroscopy (UPS) measurements [5]. The comparison allows to assign the measured signals to specific molecular orbitals, providing a self consistent validation of the experimental results. Furthermore, the calculations provide the IPs of orbitals that could not be measured, experimentally.

Unfortunately, gas phase measurements were not possible in the experiment because of the

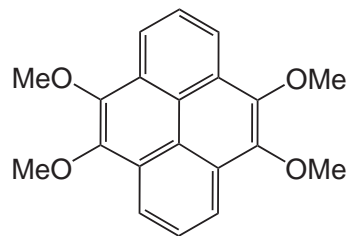
small amount of material available (a few milligrams). Instead, UPS measurements had been performed on PAH multilayers on a Au surface. As the molecules are preferentially planar to the surface while measurements are made in the perpendicular direction σ -type orbitals could not be measured in practice. In the numerical study all orbitals can be investigated so that the respective IPs become accessible. In general, the IPs of PAHs adsorbed on a metal surface are shifted by a constant energy value with respect to the gas phase results. The discrepancy stems from the photo-hole screening induced by the image charge in the metal [5]. A similar effect occurs in multilayer films in which the screening is induced by the neighboring molecules. The energy shift between the theoretical results that corresponds to isolated molecules or the dilute gas phase and the measurements on the condensed multilayers can be taken into account by adjusting the HOMO levels of both systems. Applying this energy shift to all IPs must provide a good correspondence between the experimentally measurable orbitals and the theoretical results, which serves as a useful consistency check of both measurement and calculation. For the given set of molecules the energy shift is very small so that the IP results for isolated molecules and those in the multilayer can be compared directly.

Coronene has a high symmetry (D_{6h}), a small band gap and the right size for processing techniques. Therefore, coronene and its derivatives are promising for applications like molecular electronics optoelectronics or sensors [10–13]. Kato *et al.* [14] also predicted superconductivity of coronene in a charge transfer configuration. In this article, properties of hexamethoxycoronene (HMC) and coronene-hexaone (CHO) are studied. The functional groups are tailored such that HMC is a donor while CHO is an acceptor molecule. Furthermore, calculations of tetramethoxypyrene (TMP) and pyrene-tetraone (PTO) have been performed and compared with experimental results. These poly aromatic molecules have a different symmetry and structure in comparison with coronene based molecules, which makes a comparison of these two families instructive. Calculation of tetracyanoquinodimethane (TCNQ), a well-known classical acceptor, is used as a benchmark for the calculations of the acceptor molecules. All investigated molecules are shown in Figure 1. Electronic structures of the donor and acceptor molecules are theoretically studied by B3LYP/6-31G(d) level of theory and compared with the ultraviolet photoemission spectroscopy (UPS) measurements that were carried out in parallel [5]. Electron binding energies or ionization potentials of molecules are calculated with the delta self consistent field (Δ SCF) method using the B3LYP hybrid functional.

Donors

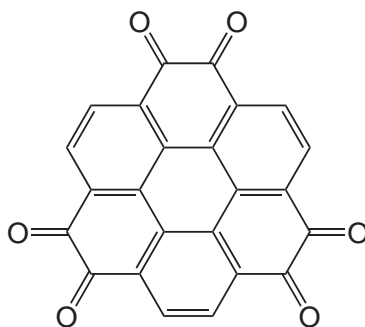


Coronene : R = H
Hexamethoxycoronene (HMC) : R = OCH₃

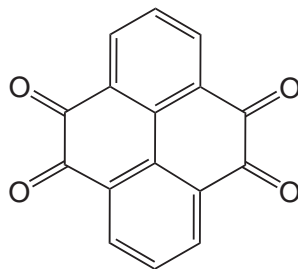


Tetramethoxypyrene (TMP)

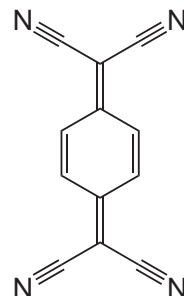
Acceptors



Coronene-hexaone (CHO)



Pyrene-tetraone (PTO)



Tetracyanoquinodimethane (TCNQ)

FIG. 1. Structure of the donor and acceptor molecules studied in this work.

II. COMPUTATIONAL DETAILS

The calculations were performed using the Gaussian03 code [15] and visualized by VMD [16]. Calculations were carried out with the B3LYP hybrid functional [17]. This combination of functionals combine the Becke's three parameter exchange potential [18, 19] with the correlation functionals of Lee-Yang-Parr [20, 21] and Vosko-Wilk-Nusair [22]. B3LYP is one of the often employed hybrid functionals [23] used in theoretical studies of molecules.

The standard 6-31G(d) basis set [24] is employed for geometry optimizations and energy calculations. This level of theory ensures a reliable estimate of structural, energetic and spectro-

scopic parameters for PAHs, which requires an extremely high computational effort for the large molecules.

Electron binding energies or ionization potentials of molecules are calculated by the delta self-consistent field (Δ SCF) method applied together with the B3LYP hybrid functional. Vertical ionization potentials are calculated using Δ SCF method in order to compare with UPS data in which vertical ionization potentials (IP_v) are measured. In IP_v final and ground state have the same geometry. First vertical ionization potentials ($IP_{v,1}$) are calculated as the difference in total energy between a molecule and its radical cation at the former geometry. For the higher ionization energies ($IP_{v,1+n}$), the energy difference (ΔE) between $IP_{v,1}$ and the HOMO energy is added to the energy of next higher orbitals ε_{HOMO-n} as a uniform shift [25–27].

$$IP_{v,1} - |\varepsilon_{HOMO}| = \Delta E \quad (1)$$

$$|\varepsilon_{HOMO-n}| + \Delta E = IP_{v,1+n} \quad (2)$$

According to Eq. 2 the eigenvalue of the HOMO-n orbital should be used in order to calculate the electron binding energy (BE) of HOMO-n. A standard view expressed in the literature for Kohn-Sham (KS) orbital energies of the occupied molecular orbitals lower than HOMO, is that they are merely auxiliary quantities. However, several authors have pointed to the interpretative power of KS orbitals in traditional qualitative molecular orbital schemes [27–30], and KS orbitals also show a uniform shift with respect to ionization energies [27, 31]. In this sense, B3LYP with its exact Hartree-Fock exchange contribution leads to better description of ionization energies by reducing the related shift [30].

The B3LYP/6-311++G(d,p) level of theory was implemented on both the anion and the neutral species for the electron affinity calculations. In case of an anionic final state, the usage of diffuse function is crucial to ensure the accuracy of the calculation. The spin unrestricted B3LYP (UB3LYP) is employed in which species are ionized with an open-shell doublet (one unpaired electron) electron configuration. Spin contamination is found in accepted limits for the open shell systems, with $\langle S^2 \rangle$ values of about 0.75-0.78 in all cases. At the stationary points a vibrational frequency calculation is performed for each numerically optimized structure to confirm that it is located at the minimum of the potential energy surface.

The results obtained with the Δ SCF method are compared with Hartree-Fock calculations based on the traditional Koopmans’ theorem approach [32]. According to Koopmans’ theorem, the ionization potential (IP) is the sign-reversed orbital energy of Hartree-Fock eigenvalues: $IP \approx$

$-E_{HOMO}$. Although KT is based on some simplification, it shows a reasonable agreement with experimental data in several cases [33]. Koopmans' theorem neglects the relaxation effect by using the frozen-orbital approximation. However, this error is frequently compensated by the oppositely directed error due to the electron correlation effect, neglected in the Hartree-Fock (HF) method. Therefore, the Koopmans' theorem is a crude but useful and fast approach [33].

Moreover, eigenvalues based on B3LYP/6-311++G(d,p) are used to estimate HOMO-LUMO gaps and LUMO energies. HOMO-LUMO gap based on the energy difference between the HOMO and LUMO eigenvalues are compared with the measured optical gaps. TD-B3LYP/6-31G(d) is also used to estimate the optical band gap (referring to the singlet excited state). As shown by Zhang *et al* the first excitation energy from TD-B3LYP calculations leads to a good prediction of the optical gap for most of the DFT methods [34]. Moreover, HOMO-LUMO gaps obtained with TD-DFT are not very sensitive to the basis set and it is shown that 6-31G(d) can show reasonable agreement for optical properties with the experimental results for the hydrocarbon molecules [34–36]. The energy difference between the HOMO and LUMO eigenvalues and TD-DFT show the similar results and both are in an excellent agreement with the experimental results.

III. RESULTS AND DISCUSSION

The result and discussion section is divided into six parts. The first part is about the experimental setup in UPS. In the second part, the symmetry of molecules and consequences of orbital symmetries on the UPS experiment are described. The effect of functional groups on coronene and pyrene derivatives is described in the third part. In the following two parts, experimental and theoretical results of the binding energies for coronene and pyrene derivatives are presented. In the sixth part, the calculated LUMO and electron affinity (EA) values for the studied compounds are discussed.

A. UPS measurements

Since only small amounts of the new molecules were available, UPS measurements have not been performed on molecules in the gas phase but on UHV-deposited molecules forming some multilayers on a Au surface. In the measurement, the work function of a clean Au surface increases significantly if the acceptor TCNQ or coronene-hexaone is adsorbed [5]. It can be understood in

terms of a partial charge transfer from the metal surface to the first molecular layer thus forming the interface dipole with its negative side pointing toward the organic film. Opposite behavior is observed for the donors HMC, TMP and coronene. The decrease of the work function of about 0.5 eV indicates the Pauli push-back effect leading to a push-back of the split-out electrons and thus to a reduction of the surface dipole of the metal. In practice, due to charge transfer between molecules and surface, the polar metal-organic interfaces change the work function and thus the binding energies with respect to vacuum level.

The binding energies in condensed films of the studied acceptors and donors (Fig. 1) are measured by UPS [5]. In the UPS spectra the signals derived from the occupied frontier orbitals of the organic overlayer are referenced to the Fermi energy of the Au substrate. By adding the value for the work function of the molecular film, the binding energies are referenced to the vacuum level. An acceptor molecule in direct contact with a metal surface may form a negatively charged species as was found for TCNQ on Ni(111) [37]. TCNQ on Au, on the other hand, was found to be almost neutral [38] because its acceptor character does not suffice to form a strong charge-transfer complex with Au, which is the metal with the highest Pauling electronegativity. For coronene on a Au surface an ionization potential of $IP=7.1$ eV is measured (see Table I) which is very close to the reported value of 7.29 eV for coronene in the gas phase [39]. As a result, one has that the Au surface shows neutrality with respect to both donor (coronene) and acceptor (TCNQ) molecules and experimental and theoretical IP values can be compared without considering a large energy shift.

The following work function values have been measured for films with a thickness of several layers deposited on Au: coronene-hexaone (5.6 eV), hexamethoxycoronene (4.8 eV), coronene (4.8 eV), tetramethoxypyrene (4.9 eV) and TCNQ (5.9 eV).

Electron binding energies for the molecular orbitals (MOs) can be extracted from the UPS spectra by assigning peak positions of the spectra, but one by one assignment for all UPS signals is not possible since in some cases they result from superposition of several occupied molecular orbitals with closely spaced binding energies. However, in most cases the HOMO signal is well separated from the deeper-lying levels and can be evaluated with high precision.

B. Symmetry analysis

For the analysis and comparison of UPS data with the calculated ionization potentials, the symmetry of the molecular orbitals must be extracted. σ or π symmetry is determined, followed by related degeneracy (E, A, ...). This information is shown in Figure 2 for the frontier orbitals and in Table I and II for the lower lying orbitals of studied molecules.

Having π symmetry is essential in order to observe the orbital in UPS. The oxygen-derived σ states appear only weakly in photoelectron spectroscopy because of the lower cross section of O-2*p* in comparison with carbon π at the photon energy (21.2 eV) used in the experiment [40, 41]. Another reason for the weak σ -derived signals in the experiment might be that the molecules are predominantly oriented parallel to the surface and the UPS spectrometer probes the normal emission direction. Electronic structure calculations allow to determine the electron binding energies of the σ -type orbitals, which are not accessible in the experiment. This way a detailed picture of the electronic structures of donor and acceptor molecules is available. Orbital symmetries with σ and π character of MOs are listed in Tables I, II and Figure 2.

Coronene and its derivatives have a degeneracy of two for the HOMO and all orbitals with E symmetry because of more than a 2-fold axis (coronene has 6-fold and HMC and CHO have 3-fold axis). CHO and HMC have a doubly degenerated HOMO with a π characteristic as depicted in Figure 2. For HMC and TMP there is no symmetry plane, so σ and π orbitals are not clearly distinguishable for the lower lying orbitals. However, they are reported according to major contribution of σ - or π -type symmetry in the orbital's notations in Tables I and II.

Pyrene derivatives and TCNQ have a non-degenerate orbital because of the 2-fold axis. Pyrene-tetraone (PTO) has an exceptional situation because HOMO and HOMO-1 have σ -type symmetry and are in-plane as shown in Figure 1. Therefore, they are not traceable in UPS because of the low cross section of O-2*p* since these MOs are located mainly on the oxygen atoms (see Figure 2). For PTO, reliable UPS binding energies could not be determined due to charging.

To sum up, a survey of Tables I and II reveals that the presence of O atoms and cyanid groups increases the σ -type part of the occupied orbitals of acceptor molecules. Thus, acceptors have more σ -symmetry orbitals near the HOMO. The experimentally inaccessible σ -type orbitals are provided by the electron structure calculations as shown in Tables I, II.

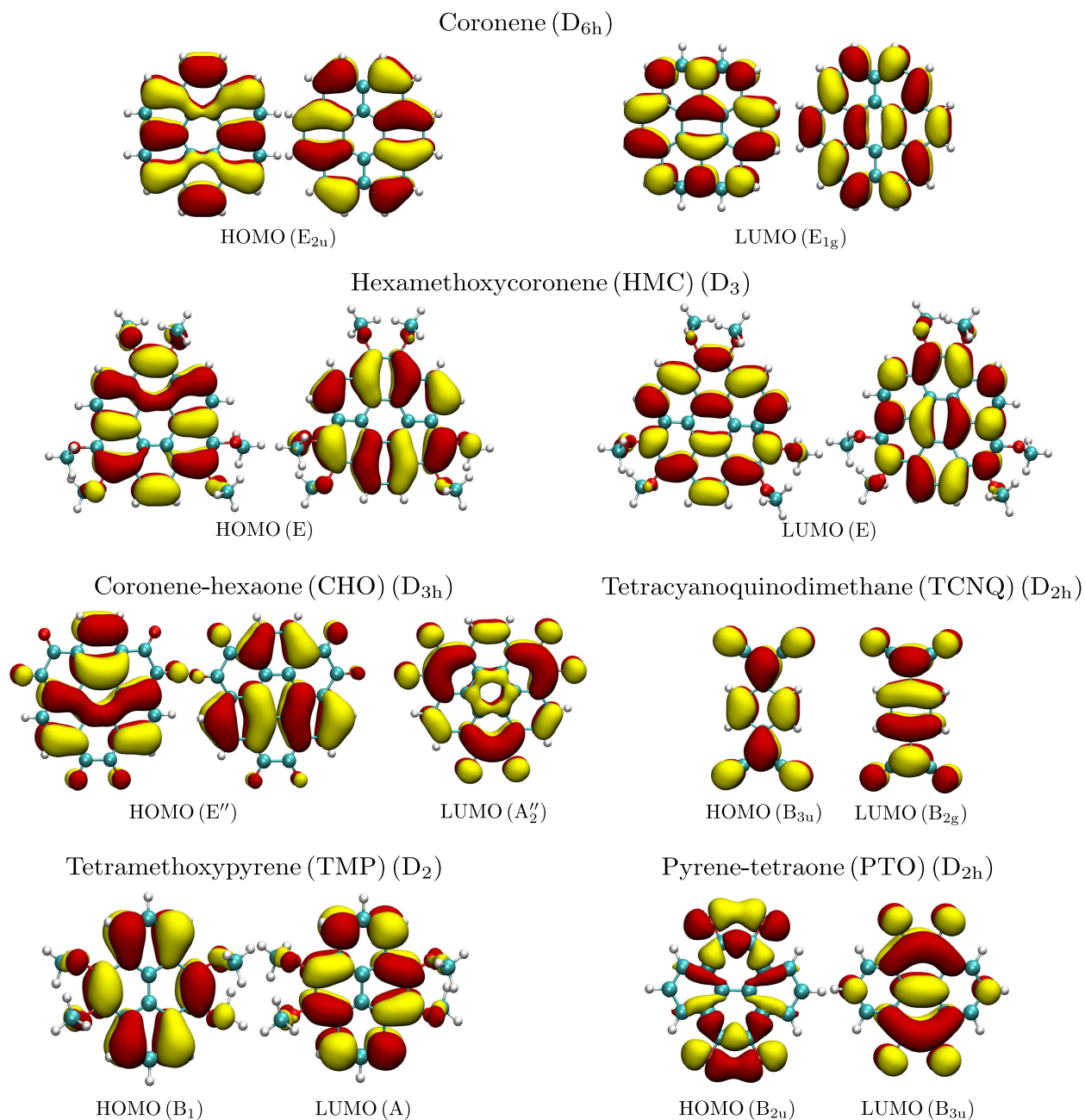


FIG. 2. HOMO and LUMO orbitals computed for the studied molecules. The symmetry of each molecule and the symmetry of the related molecular orbitals are shown in parentheses. Among all PAHs donor and acceptor molecules just PTO has a σ -type HOMO orbital. All the coronene derived molecules show a doubly degenerate HOMO.

C. Effect of functional groups

The electron-withdrawing carbonyl groups of CHO and PTO reduce the charge density in the π system, while in HMC and TMP, electrons are donated to the π system by the methoxy (OMe) groups. Therefore, the aromatic rings in CHO and PTO are positively charged, while the methoxy substituted molecules are negatively charged. Thus, CHO is an acceptor in comparison with coronene and HMC, and PTO is an acceptor compared to TMP.

The bond lengths of CHO along the symmetry plane are distinctly larger than those of coronene. The first C–C bond length at the edge of the double bonded oxygen atoms increases from 1.37 Å (coronene) to 1.54 Å for CHO. The other bond lengths increase by about 0.02 Å with respect to coronene. For CHO, all the bond lengths inside the aromatic ring are larger than those in HMC and coronene. In HMC, the C–C bond lengths are of the same size as those of coronene, but Mulliken population shows that the C atoms of the aromatic rings are slightly more charged compared to coronene. In principle, the similar behavior is found for TMP and PTO.

Donor and acceptor molecules are best investigated by analyzing the molecular orbitals. Any change in the functional groups of the molecules will be reflected in the binding energies and the molecular orbital energies. Therefore, evaluation of molecular orbitals shows how the functional groups tune the electronic structure. Also, with the help of ab-initio calculations one can analyze details of the electronic structure and in particular σ orbitals which are not accessible by UPS measurement. Also underlying orbital structure of overlapping UPS signals can be analyzed by the calculation.

D. Electron binding energies of coronene derivatives

Theoretical and experimental binding energies of coronene and its derivatives coronene-hexaone (CHO) and hexamethoxycoronene (HMC) are listed in Table I. A survey of Table I reveals that vertical electron binding energies (IPs) calculated in Δ SCF-B3LYP approximation are, on the whole, in good agreement with the corresponding experimental IPs. Calculations based on the Δ SCF method correspond to the vertical IP of the molecules in the gas phase. In general, they may differ from measurements of condensed layers on a metal surface by a constant energy value. As shown in Table I the energy shift between the multilayer measurements and the calculations corresponding to the gas phase are very small, which corresponds to the fact that the

IP=7.1 eV of coronene on Au is close to the reported gas phase value IP=7.29 eV [39].

For coronene and the derivatives the Koopmans' energies for the HOMO differ by less than 0.5 eV from the Δ SCF binding energies. For the deeper-lying orbitals, the Koopmans' energies are too large in comparison with Δ SCF and experimental results. This deviation is caused by correlation and relaxation effects which are neglected in Koopmans' theorem. For comparison, results from Koopmans' theorem are presented for HMC in Table I. For coronene and CHO deviations of the Koopmans' energies are of the same order of magnitude. Note that the σ -like orbitals of CHO appear only very weakly in UPS spectra. Δ SCF-B3LYP results can cover a wide range of MOs and show good agreement with the UPS data.

The first ionization potential (binding energy of HOMO) of HMC is shifted up by 0.5 eV in

TABLE I. Electron binding energies (eV) for coronene and its derivatives with the symmetry labels calculated by B3LYP/6-31G* and compared to vertical excitation energies from ultra violet photoelectron spectroscopy (UPS) and Koopmans' theorem (KT).

MOs	CHO(D _{3h})			HMC(D ₃)				Coronene(D _{6h})		
	Symm.	Δ SCF	UPS	Symm.	KT	Δ SCF	UPS	Symm.	Δ SCF	UPS
HOMO	E''(π)	8.78	8.8	E(π)	6.86	6.41	6.5	E _{2u} (π)	6.84	7.1
HOMO-1	E'(σ)	8.80	E(π)	8.74	7.66	} 7.9	E _{1g} (π)	8.11	} 8.8
HOMO-2	A' ₁ (σ)	8.82	A ₂ (π)	9.25	7.80		B _{2g} (π)	8.56	
HOMO-3	A'' ₁ (π)	9.23	A ₁ (π)	9.44	8.15		B _{1g} (π)	8.62	
HOMO-4	E'(σ)	10.05	E(σ)	11.03	8.38	A _{2u} (π)	9.84
HOMO-5	A' ₂ (σ)	10.11	A ₁ (σ)	11.59	8.51	E _{2g} (σ)	9.94
HOMO-6	E''(π)	10.33	} 10.3	E(π)	11.65	9.11	} 9.3	E _{2u} (π)	10.25
HOMO-7	A'' ₂ (π)	10.70		A ₂ (π)	11.65	9.17		B _{2u} (σ)	11.09
HOMO-8	E''(π)	11.80	A ₂ (π)	12.47	9.52		E _{1u} (σ)	11.13
HOMO-9	E'(σ)	11.84	E(π)	12.64	9.71	A _{2g} (σ)	11.54
HOMO-10	A'' ₁ (π)	12.37	E(π)	12.94	9.95	B _{1u} (σ)	11.55

comparison to coronene. As displayed in Table I, hexamethoxycoronene has three main signals in the experimental spectrum below 10 eV [5]. The first of them at 6.5 eV is the HOMO with π -like symmetry with the double degenerate representation E (Figure 2). The calculation yields a binding energy (Δ -SCF) of 6.41 eV in excellent agreement with the photoelectron spectra. The calculated

binding energy of electrons in the HOMO of HMC is about 0.4 eV lower than that of coronene due to the six methoxy groups on the periphery which increase the charge density in the π system. The effect of the methoxy groups is weaker than that of electron-withdrawing keto groups of CHO since the methoxy groups contain the electron-donor methyl and the acceptor oxygen which partially compensate each other. There are three pairs of methoxy groups in the ring system and each pair is in trans configuration (see Figure 1 and 2). The methoxy groups can easily rotate in a solvent but this rotation will be blocked on the surface. The orientation of the methoxy group configurations has a strong influence also on the interaction between metal surface and molecule. The trans configuration of methoxy groups may reduce the contact of the aromatic ring system with the surface so that it can effectively suppress charge transfer between molecule and metal surface. The second signal in the UPS spectra appears at 7.9 eV and is assigned to the group HOMO-1, HOMO-2 and HOMO-3 all having π -like symmetry. Note that there is no strict π - and σ -type symmetry in HMC, but we can identify ' π -like' and ' σ -like' symmetry by comparison with the parent molecule coronene. HOMO-4 and HOMO-5 are very weak in the experimental spectra because they have σ -like symmetry, and contain a high contribution from oxygen 2p which has a low cross section at the photon energy (21.2 eV) used in the experiment [40, 41]. Another reason for the weak σ -derived signals in the experiment might be that the molecules are predominantly oriented parallel to the surface and the UPS spectrometer probes the normal emission direction. For perfectly parallel orientation, σ emission is forbidden by symmetry selection rules. The UPS signal at 9.3 eV corresponds to the group of the HOMO-6 to HOMO-8 states with π -like symmetry.

Coronene-hexaone (CHO) constitutes a more complicated adsorption behavior than HMC. CHO is a planar molecule with high electron affinity. The first layer being in direct contact with surface experiences a substantial charge transfer from Au showing up in terms of a new interface state [5]. For comparison with theory we refer the UPS data for higher CHO coverage, where the interface state has disappeared in the spectra. In the multilayer coverage two signals rise in the region below 11 eV. As shown in Table I, the first signal corresponds to the HOMO and appears at 8.8 eV in very good agreement with the Δ SCF calculation (8.78 eV). This value is similar to TCNQ which is a strong classical acceptor (Figure II). The binding energy of electrons in the HOMO of CHO has increased by more than 2 eV with respect to coronene because of the electronegative keto groups. HOMO-1 and HOMO-2 as well as HOMO-4 and HOMO-5 are weak signals in the experimental spectra since they are derived from the oxygen 2p_{x,y} orbitals that are

aligned in the molecular plane. HOMO-6 and HOMO-7 (π symmetry) constitute the second UPS signal at 10.3 eV in the measured spectra. The Δ SCF calculation again shows good agreement. Obviously the six carbonyl groups strongly alter the electronic structure of CHO compared to unfunctionalized coronene, and make CHO a strong acceptor.

E. Binding energies of pyrene derivatives

For **tetramethoxy**pyrene (TMP) and **tetracyanoquinodimethane** (TCNQ), the theoretical binding energies are smaller than the experimental values. For the HOMO of TMP the difference is 0.42 eV, similar as for the overlapping HOMO-1 and HOMO-2 signals. HOMO-3 to HOMO-4 and HOMO-9 to HOMO-10 have σ -like symmetry and appears weakly in the experimental spectra due to a large oxygen 2p content. The π -like group HOMO-6 to HOMO-8 can not be resolved experimentally and shows up as one signal centered at 9.2 eV.

TABLE II. Same as table I, but for pyrene derivatives and TCNQ.

MOs	PTO(D _{2h})			TMP(D ₂)			TCNQ(D _{2h})		
	Symm.	Δ SCF	UPS	Symm.	Δ SCF	UPS	Symm.	Δ SCF	UPS
HOMO	B _{2u} (σ)	8.70	B ₁ (π)	6.18	6.7	B _{3u} (π)	8.87	9.3
HOMO-1	A _g (σ)	8.90	B ₃ (π)	7.09	} 7.7	B _{1g} (π)	10.49	} 10.8
HOMO-2	B _{2g} (π)	8.92	B ₂ (π)	7.30		B _{2g} (π)	10.91	
HOMO-3	A _u (π)	9.50	A (π)	8.03	B _{3g} (σ)	11.56
HOMO-4	B _{1g} (π)	9.67	B ₃ (σ)	8.06	B _{2u} (σ)	11.58
HOMO-5	B _{3g} (σ)	9.96	A(π)	8.28		A _u (σ)	11.87
HOMO-6	B _{1u} (σ)	10.26	B ₁ (π)	8.66	} 9.3	B _{1g} (π)	11.88
HOMO-7	B _{3u} (π)	10.60	B ₂ (π)	8.72		B _{1u} (π)	11.89
HOMO-8	B _{2g} (π)	11.66	B ₂ (π)	8.96		A _g (σ)	12.01
HOMO-9	B _{3g} (σ)	12.08	B ₁ (π)	9.42	B _{3g} (σ)	12.34
HOMO-10	A _g (σ)	12.10	B ₂ (σ)	9.71	B _{2u} (σ)	12.38

For **pyrene-tetraone** (PTO) reliable UPS binding energies could not be determined due to charging. Moreover, the HOMO has σ symmetry and is thus not observable in the UPS experiment.

Charging was also observed for thick CHO films (above 10 nm thickness). For TCNQ, HOMO-1 and HOMO-2 agree fairly well with the experimental signal centered at 10.6 eV. HOMO-3 to HOMO-5 have σ symmetry and appear only weakly in UPS spectra.

F. LUMO and electron affinity

The strength of an acceptor molecule is measured by its electron affinity (EA) which is the energy released when adding one electron to the lowest unoccupied molecular orbital. An acceptor must have a high electron affinity, while low electron affinity is required for effective donor molecules. Since EA depends on the lowest unoccupied molecular orbital (LUMO), it can be calculated more accurately by considering the final state (anion). In order to describe the anion with an extra electron sufficiently, a diffuse basis set is required. We use the B3LYP/6-311++G(d,p) basis to study donor and acceptor molecules.

The calculated EA of coronene is 0.48 eV which is in good agreement with the reported experimental value of 0.470 ± 0.009 eV [42]. A high electron affinity is the major characteristic of strong acceptors like TCNQ. Reported values for the EA of TCNQ vary with the applied measurement technique [43–46]. Calculations values of EA are in the range of 3.4 ± 4 eV [47]. Using B3LYP/6-311++G**, we obtained an EA of 3.62 eV, while B. Milián et al. report a value of 3.42 eV calculated with B3LYP/cc-pVDZ and 3.28 eV calculated with CCSD/aug-cc-pVDZ. All these values are close to the reported experimental value of $EA = 3.3 \pm 3$ [44, 46].

The electron affinity of CHO is 3.5 eV (see first column of Table III) which is close to the electron affinity of TCNQ (3.62 eV). Therefore CHO is expected to be a strong electron acceptor. CHO has a large electron affinity and an extended π system which makes it an interesting alternative to common acceptors.

In Table III the experimental gaps are compared with the theoretical gaps. To estimate the optical gap, both TD-DFT and the difference of B3LYP HOMO-LUMO eigenvalues are used and the results are listed in the second and third column of Table III respectively. In the case of large molecules there is a good agreement between the eigenvalue differences and the measured optical gap. In the earlier study, it is shown that there is a large deviation between the calculated gap using B3LYP and experimental results [33]. In the same paper, discrepancy depends to the size of molecule and it decreases by increasing the size of hydrocarbons. Therefore, one can conclude the good agreement in our calculations should be attributed to the large size of the hydrocarbons.

TABLE III. Δ SCF electron affinity (EA) using 6-311++G** basis set. Moreover the HOMO-LUMO gaps are calculated using TD-DFT/6-31G* (singlet excitation), second column and B3LYP/6-311++G** (LUMO-HOMO eigenvalue differences) third column. All values are given in eV.

Molecule	EA (B3LYP)	EA (Exp)	Gap (TD-DFT)	Gap ($\epsilon_{LUMO} - \epsilon_{HOMO}$)	Gap (Exp)
Coronene	0.48	0.47 ^a	3.99	3.23	3.54 ^c
Coronene-Hexaone	3.50	...	2.98	2.57	3.20 ^c
Hexamethoxycoronene	0.51	...	3.81	3.09	3.30 ^c
Pyrene-Tetraone	2.48	...	3.48	2.22	
Tetramethoxypyrene	0.41	...	3.67	3.58	
TCNQ	3.62	3.3 ^b	3.04	2.54	3.10 ^d

^a Ref [42]

^b Ref [44, 46]

^c Ref [11]

^d Ref [48]

For all compounds, the calculated HOMO-LUMO eigenvalue differences are smaller than the measured gaps. The gaps obtained from TD-DFT are spread symmetrically around the experimental values. In general, the calculated gaps from TD-DFT and the HOMO-LUMO eigenvalues deviate less than 20% from the experimental gaps, which is a reasonable result for this quantity. The fair agreement between the experimental values and the results calculated with B3LYP/6-31G* indicates that this calculation method may be used also for the larger molecules of this family called nanographene for which more correlated methods like post Hartree-Fock or even DFT with the diffuse basis sets are difficult or not applicable.

IV. SUMMARY

In this paper, we have reported theoretical and experimental electron binding energies of different MOs for coronene, pyrene and their methoxy and keton-derivatives as polycyclic aromatic hydrocarbons and compared them with TCNQ as a well-known classical acceptor. The studied compounds demonstrate how the functional groups can tune the molecules' electronic state, providing moderate donor or strong acceptor properties.

Comparison of electron structure calculations and photoelectron spectroscopy data provides new insights into the electronic structure of the new compounds. The calculated molecular orbitals have been used to identify and complement the experimental results. UPS measurements

of the compounds on a Au surface provide IPs in an agreement with experimental and calculated values for the gas phase. The absence of an energy shift, induced by the metal substrate or the neighboring molecules, is so far not understood, but the good agreement between the various UPS signals and the calculated π -type orbitals demonstrates the direct comparability of the molecule's IPs in the condensed and the gas state. In fact, Δ SCF-B3LYP reproduces the whole range of IPs in the measured UPS spectra, while Koopmans' theorem shows a good agreement just for the first IP. The calculated electron affinities allow to rate the donor or acceptor character of the molecules. They confirm that CHO is a strong acceptor. Its high electron affinity (3.5 eV), which characterizes a good acceptor, is almost as large as the affinity of TCNQ (3.62 eV). HMC, coronene and TMP with their low ionization potentials and rich aromatic systems are suitable candidates for donors. HMC is an appropriate choice for surface applications due to its trans isomerism. Especially interesting for the formation of charge transfer complexes are the molecules CHO and HMC. Our results show that they are good acceptor and donor molecules, respectively, and with their coronene centers they have a very similar molecular structure. This is analogous to the TTF-TCNQ pair with the benzene core which is studied since a long time. The proposed coronene-based donor-acceptor molecules could be the starting point of a new generation of charge transfer salts based on molecular nanographenes.

V. ACKNOWLEDGMENTS

Financial support by the Deutsche Forschungs Gemeinschaft DFG through the Collaborative Research Center "Condensed Matter Systems with Variable Many-Body Interactions" (Transregio SFB/TRR 49), the graduate school of excellence MAINZ as well as the center COMATT are gratefully acknowledged.

-
- [1] E. Coronado, P. Delhaès, D. Gatteschi, and J. S. Miller, *Molecular magnetism: from molecular assemblies to the devices* (Springer, 1996).
 - [2] T. Ishiguro, K. Yamaji, and G. Saito, *Organic superconductors* (Springer, 1998).
 - [3] A. M. Kini, U. Geiser, H. H. Wang, K. D. Carlson, J. M. Williams, W. K. Kwok, K. G. Vandervoort, J. E. Thompson, and D. L. Stupka, *Inorg. Chem.* **29**, 2555 (1990).

- [4] H. S. Nalwa, *Handbook of Organic Conductive Molecules and Polymers*, Vol. 1 (John Wiley and Sons, 1997).
- [5] K. Medjanik, D. Kutnyakhov, S. A. Nepijko, G. Schönhense, S. Naghavi, V. Alijani, C. Felser, R. Rieger, M. Baumgarten, and K. Müllen, *Phys. Chem. Chem. Phys.* **12**, 7184 (2010).
- [6] A. van de Craats, N. Stutzmann, O. Bunk, M. Nielsen, M. Watson, K. Müllen, H. Chanzy, H. Siringhaus, and R. Friend, *Adv. Mater.* **15**, 495 (2003).
- [7] S. Xiao, J. Tang, T. Beetz, X. Guo, N. Tremblay, T. Siegrist, Y. Zhu, M. Steigerwald, and C. Nuckolls, *J. Am. Chem. Soc.* **128**, 10700 (2006).
- [8] A. F. Garito and A. J. Heeger, *Acc. Chem. Res.* **7**, 232 (1974).
- [9] J. Wu, W. Pisula, and K. Müllen, *Chem. Rev.* **107**, 718 (2007).
- [10] U. Rohr, P. Schlichting, A. Böhm, M. Gross, K. Meerholz, C. Bräuchle, and K. Müllen, *Angew. Chem.* **37**, 1434 (1998).
- [11] R. Rieger, M. Kastler, V. Enkelmann, and K. Müllen, *Chem. Eur. J.* **14**, 6322 (2008).
- [12] T. Suzuki, J. Levy, and J. T. Y. Jr., *Nano Lett.* **6**, 138 (2006).
- [13] V. Casagrande, A. Alvino, A. Bianco, G. Ortaggi, and M. Franceschin, *J. Mass. Spectrom.* **44**, 530 (2009).
- [14] T. Kato and T. Yamabe, *J. Chem. Phys.* **117**, 2324 (2002).
- [15] M. J. Frisch, G. W. Trucks, H. B. Schlegel, G. E. Scuseria, M. A. Robb, J. R. Cheeseman, J. A. Montgomery, Jr., T. Vreven, K. N. Kudin, J. C. Burant, J. M. Millam, S. S. Iyengar, J. Tomasi, V. Barone, B. Mennucci, M. Cossi, G. Scalmani, N. Rega, G. A. Petersson, H. Nakatsuji, M. Hada, M. Ehara, K. Toyota, R. Fukuda, J. Hasegawa, M. Ishida, T. Nakajima, Y. Honda, O. Kitao, H. Nakai, M. Klene, X. Li, J. E. Knox, H. P. Hratchian, J. B. Cross, V. Bakken, C. Adamo, J. Jaramillo, R. Gomperts, R. E. Stratmann, O. Yazyev, A. J. Austin, R. Cammi, C. Pomelli, J. W. Ochterski, P. Y. Ayala, K. Morokuma, G. A. Voth, P. Salvador, J. J. Dannenberg, V. G. Zakrzewski, S. Dapprich, A. D. Daniels, M. C. Strain, O. Farkas, D. K. Malick, A. D. Rabuck, K. Raghavachari, J. B. Foresman, J. V. Ortiz, Q. Cui, A. G. Baboul, S. Clifford, J. Cioslowski, B. B. Stefanov, G. Liu, A. Liashenko, P. Piskorz, I. Komaromi, R. L. Martin, D. J. Fox, T. Keith, M. A. Al-Laham, C. Y. Peng, A. Nanayakkara, M. Challacombe, P. M. W. Gill, B. Johnson, W. Chen, M. W. Wong, C. Gonzalez, and J. A. Pople, "Gaussian 03, Revision C.02, Gaussian, inc., wallingford, CT," (2004).
- [16] W. Humphrey, A. Dalke, and K. Schulten, *Journal of Molecular Graphics* **14**, 33 (1996).
- [17] P. J. Stephens, F. J. Devlin, C. F. Chabalowski, and M. J. Frisch, *J. Phys. Chem.* **98**, 11623 (1994).

- [18] A. D. Becke, *J. Chem. Phys.* **98**, 5648 (1993).
- [19] A. D. Becke, *J. Chem. Phys.* **98**, 1372 (1993).
- [20] R. G. Parr and Y. Weitao, *Density-functional theory of atoms and molecules* (Oxford University Press, Oxford, 1989).
- [21] C. Lee, W. Yang, and R. G. Parr, *Phys. Rev. B* **37**, 785 (1988).
- [22] S. H. Vosko, L. Wilk, and M. Nusair, *Can. J. Phys.* **58**, 1200 (1980).
- [23] P. E. M. Siegbahn, *Faraday Discuss.* **124**, 289 (2003).
- [24] P. Hariharan and J. Pople, *Theoret. Chimica Acta* **28**, 213 (1973).
- [25] P. R. N. Kama and H. M. Muchall, *J. Phys. Chem. A* **112**, 13691 (2008).
- [26] H. M. Muchall and N. H. Werstiuk, *Can. J. Chem.* **84**, 1124 (2006).
- [27] D. P. Chong, O. V. Gritsenko, and E. J. Baerends, *J. Chem. Phys.* **116**, 1760 (2002).
- [28] W. Kohn, A. D. Becke, and R. G. Parr, *J. Phys. Chem.* **100**, 12974 (1996).
- [29] E. J. Baerends and O. V. Gritsenko, *J. Phys. Chem. A* **101**, 5383 (1997).
- [30] R. Stowasser and R. Hoffmann, *J. Am. Chem. Soc.* **121**, 3414 (1999).
- [31] C.-G. Zhan, J. A. Nichols, and D. A. Dixon, *J. Phys. Chem. A* **107**, 4184 (2003).
- [32] T. Koopmans, *Physica* **1**, 104 (1933).
- [33] U. Salzner, J. B. Lagowski, P. G. Pickup, and R. A. Poirier, *J. Comput. Chem.* **18**, 1943 (1997).
- [34] G. Zhang and C. B. Musgrave, *J. Phys. Chem. A* **111**, 1554 (2007).
- [35] D. Majumdar, H. M. Lee, J. Kim, K. S. Kim, and B. J. Mhin, *J. Chem. Phys.* **111**, 5866 (1999).
- [36] A. E. Clark, *J. Phys. Chem. A* **110**, 3790 (2006).
- [37] J. Giergiela, S. Wellsa, T. Landa, and J. C. Hemmingera, *Surface Science* **255**, 31 (1991).
- [38] I. F. Torrentea, K. J. Frankea, and J. I. Pascual, *International Journal of Mass Spectrometry* **277**, 269 (2008).
- [39] E. Clar, J. M. Robertson, R. Schloegl, and W. Schmidt, *J. Am. Chem. Soc.* **103**, 1320 (1981).
- [40] G. C. Angel and J. A. R. Samson, *Phys. Rev. A* **38**, 5578 (1998).
- [41] D. Toffoli and R. R. Lucchese, *J. Chem. Phys.* **120**, 6010 (2004).
- [42] M. A. Duncan, A. M. Knight, Y. Negishi, S. Nagao, Y. Nakamura, A. Kato, A. Nakajima, and K. Kaya, *Chem. Phys. Letters* **309**, 49 (1999).
- [43] C. E. Klots, R. N. Compton, and V. F. Raaen, *J. Chem. Phys.* **60**, 1177 (1974).
- [44] R. M. Metzger, B. Chen, U. Hopfner, M. V. Lakshmikantham, D. Vuillaume, T. Kawai, X. Wu, H. Tachibana, T. V. Hughes, H. Sakurai, J. W. Baldwin, C. Hosch, M. P. Cava, L. Brehmer, and

- G. J. Ashwell, *J. Am. Chem. Soc.* **119**, 10455 (1997).
- [45] R. N. Compton and C. D. Cooper, *J. Chem. Phys.* **66** (1977), doi:"bibinfo doi 10.1063/1.433743.
- [46] C. Jin, R. E. Haufler, R. L. Hettich, C. M. Barshick, R. N. Compton, A. A. Puretzky, A. V. Demyanenko, and A. A. Tuinman, *Science*, 68(1994).
- [47] B. Miliana, R. Pou-Amerigo, R. Viruela, and E. Orti, *Chemical Physics Letters* **391**, 148 (2004).
- [48] H. T. Jonkmana and J. Kommandeura, *Chemical Physics Letters* **15**, 496 (1972).